Critique of interatomic potentials obtained from neutron diffraction

R. A. Aziz, M. J. Slaman, and A. R. Janzen
Department of Physics, University of Waterloo, Waterloo, Ontario, Canada N2L 3G1
(Received 12 November 1993; revised manuscript received 10 March 1994)

Fredrikze *et al.* [Phys. Rev. Lett. **62**, 2612 (1989)] constructed an interatomic potential for argon directly from a single physical property, namely, by inversion of neutron scattering data. The well depth of the potential has an assigned error of ±3%. To appraise its quality, we fit analytic functions to the experimental potential and use them to calculate certain spectroscopic values associated with the ultraviolet absorption spectrum of the argon dimer. These values are the vibrational and rotational constants of the five lowest vibrational levels of the ground state of Ar_2, values which, together with a knowledge of the second virial coefficient and long-range forces, completely define the potential well. The predictions based on these potentials and a highly accurate multiproperty potential are then compared with the experimental data. It is found that, unlike the multiproperty potential, the single-property neutron diffraction potential cannot predict these experimental spectroscopic data within experimental error. Other properties which are significantly determined by the potential well are also analyzed based on this potential. The inability of the potential to predict these additional properties reinforces our conclusion about its inadequacy as a proper characterization of the interaction.

PACS number(s): 61.12.−q, 34.20.Cf, 03.75.Dg

INTRODUCTION

In recent years, there have been a number of attempts [1–3] to determine pair interatomic potentials for inert gas systems from neutron scattering experiments. The main reason cited for doing so is to obtain "direct" experimental values for $u_2(r)$ (with error limits [2,3]), which are not influenced by the empirical mathematical form chosen to represent the interaction [2].

In brief, the static structure factor $S(\kappa)$ is measured by means of neutron scattering in a gas as a function of density ρ at fixed T. From the low-density limit $S_0(\kappa)$, the low-density limit of the pair distribution function $g_0(r)$ is obtained by simple Fourier transformation and, finally, the isotropic pair potential for the part of the well and the lower repulsive wall is determined as

$$u_2(r) = -k_b T \ln g_0(r) \ .$$

Since $S_0(\kappa)$ is extracted from experiment in a finite range of κ, some kind of extrapolation [2] must be applied to $S_0(\kappa)$ both toward zero- and high-κ values in order to perform a reliable Fourier transform. The most recent determination is that of Fredrikze *et al.* [3] for argon who increased the accuracy of their measurements of $S_0(\kappa)$ in the low-density region and extended the κ range of their measurements to $2.4 < \kappa < 100$ nm^{-1} in an attempt to avoid *ad hoc* extrapolation procedures. Their analysis was somewhat different in that they derived the pair potential from the low-density limit of the total correlation function $h_0(r)$ as

$$u_2(r) = -k_b T[\ln h_0(r) + 1] \ .$$

Fredrikze *et al.* [3] appear to "test" the accuracy of their procedure only qualitatively by comparing their results with accurate multiproperty-fitted potentials [4,5] in a smallish plot. That plot reveals that their potential is appreciably shallower (by up to ~6.5%) than all recent argon potentials [4–11].

In general, a detailed analysis of the ability of a given potential to predict a variety of experimental properties is essential in order to appraise its quality. Such an analysis will provide a more complete appreciation of both the applicability and limitations of diffraction potentials. The purpose of this paper is to present details for this analysis for the more recent argon pair diffraction potential of Fredrikze *et al.* [3].

ANALYSIS

The neutron diffraction pair potential was determined at separations only in the range $3.2 < r < 10.8$ Å, which mainly encompasses the potential well. To appraise its quality, we must consider dilute gas properties that are influenced chiefly by the potential well.

The most important of these properties is the vibration-rotation band system of Ar_2. The spectroscopic constants that have been measured are very accurate and sense *precisely* that region of the well for which the neutron scattering potential has been determined. We will concentrate chiefly on this property but will, for completeness, analyze two other properties which depend on the potential well: the glory structure (i.e., quantum undulations) in the total collision cross-section (TCCS) and the second virial coefficients.

To facilitate the analysis, analytic functions were fitted to the numerical $u_2(r)$ points of Fredrikze *et al.* [3] (dubbed here as FVVMCB] so that the predictions of properties based on this potential could be calculated. Three such analytic "mimic" potentials were actually constructed. The first two (MMS-1 and MMS-2) have the hybrid Maitland-Smith form [12], chosen because of its realistic nature and because of its convenience for the

 ©1994 The American Physical Society

mimicking procedure but without due concern about its long-range behavior (see Appendix). MMS-1 reproduces, as closely as possible, the FVVMCB in the center of its error bars. Since this potential is shallower than current state-of-the-art potentials, a second mimic was constructed (MMS-2) which reproduces, as closely as possible, the FVVMCB at its maximum allowed well depth, and yet stays within the error bars as much as possible. Although long-range forces have little influence on the spectroscopic results, a third "mimic" with a Hartree-Fock dispersion HFD-*B* form [5] (MHFD) was constructed with a van der Waals tail possessing dispersions coefficients C_6 [13], C_8 [14], and C_{10} [14] within accepted theoretical error bounds. The parameters of this potential were chosen so that it reproduces the FVVMCB potential within its error bars. (The parameters for these potentials are presented in Table I.) Predictions of the spectroscopic constants [15], the glory structure in the TCCS [16] and the second virial coefficients on the basis of the three "mimic" potentials were calculated. By way of comparison, predictions based on the latest Hartree-Fock-dispersion, individually-damped (HFDID1) potential of Aziz [11] will also be presented. This potential is currently considered to be the best characterization of the Ar-Ar interaction. Its scaling parameters are in close agreement with other model potentials but differ substantially from the FVVMCB or its mimics (see Table I). In particular, the latter have potential wells which are appreciably shallower near the bottom of the well but which become deeper at larger separations. In fact, MMS-2 is about 15% deeper than the HFDID1 near 1.6σ, where the potential is considered to be the most sensitive to neutron scattering data. A similar observation was made by Barocchi, Zoppi, and Egelstaff [2] in the case of krypton. The HFDID1 and the three mimic potentials are presented with the FVVMCB in Figs. 1 and 2.

The property which is the best discriminator of potentials is the vibration-rotation spectrum of the Ar_2 dimer as determined by *uv* absorption spectroscopy. The vibrational spacings ΔG place severe constraints on the width of the well as a function of depth below the $u_2(r)=0$ line. The rotational constants B_v allow a determination of the "effective" mean separations r_c for various vibrational levels. Therefore, ΔG and B_v together accurately define the well. Deviations of the calculated energy level spacings ΔG for four potentials from observed spacings [15] and the corresponding deviations of B_v are shown in Table II. It is seen that the HFD-*B*3 reproduces the ΔG and B_v and hence r_c quite well. However, all three mimics are much too shallow to reproduce the ΔG acceptably, as evidenced by the negative deviations. In fact, the deviation in the spacing $G(\frac{11}{2})$-$G(\frac{1}{2})$ is more than thirty-five times a conservative estimate of the experimental error.

TABLE I. Parameters for (a) analytic mimic potentials and (b) several argon potentials.

(a) Mimic potentials

	MMS-1[a]	MMS-2[b]	MHFD[a]
α_1	13.5	13.5	
α_2	13.0	13.0	
γ_1	1.0	1.0	
γ_2	7.5	1.5	
A^*			$4.273\,984\times10^6$
α^*			14.907 318
β^*			−1.274 415
c_6			1.165 802
c_8			0.674 070
c_{10}			0.413 815
D			1.695 200
C_6 [a.u.]			64.3
C_8 [a.u.]			1880.
C_{10} [a.u.]			60 900.
ϵ/k [K]	133.7	137.15	134.7
r_m [Å]	3.774	3.774	3.763
σ [Å]	3.386	3.386	3.384

(b) Argon potentials

Potential reference		ϵ/k (K)	σ (Å)	r_m (Å)
KMA	[9]	143.27	3.353	3.7545
BFW	[4]	142.095	3.361	3.7612
DSMZT	[10]	142.7	3.357	3.756
HFD-*C*	[8]	143.224	3.357	3.759
HFD-*B*2	[5]	143.224	3.353	3.7565
HFD-*B*3	[6]	143.25	3.356	3.761
HFDID1	[11]	143.235	3.350	3.757

[a]Mimic of FVVMCB, neutron diffraction potential of Ref. [3].

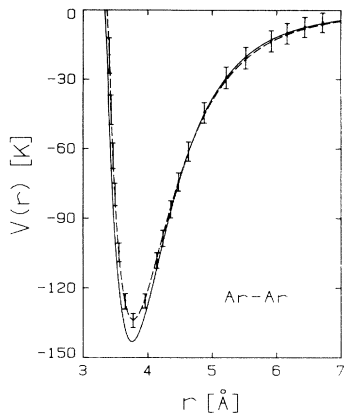

FIG. 1. Comparison of the HFDID1 (solid line) and MMS-1 (dashed line) potentials with the neutron scattering FVVMCB potential (large dots with error bars).

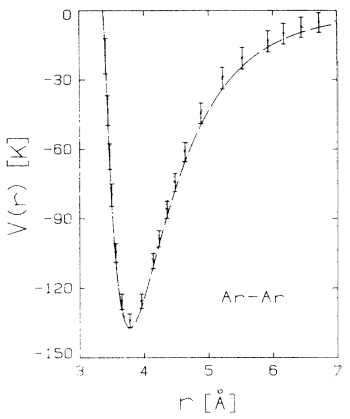

FIG. 2. Comparison of the MMS-2 (dash-dotted line) and MHFD (dotted line) potentials with the neutron scattering FVVMCB potential (large dots with error bars).

In addition, the small calculated values of B_v compared with experiment imply values of the "effective" mean separations r_c, which are *too large* for all the mimic potentials in general and the MMS-2 in particular. From this, we can infer that the well of the MMS-2 potential at the point where its outer attractive wall is located at $r=1.6\sigma$ is *too wide*. This indicates that MMS-2, which is 15% deeper than currently accepted potentials at $r=1.6\sigma$ [$u_{\text{MMS-2}}(1.6\sigma)=-27.7$ K] is *too deep* precisely where the potential is considered to be the most sensitive to neutron scattering data. Additional confirmation of this conclusion stems from a theoretical analysis of the potential at this separation. At $r=1.6\sigma$, the self-consistent field contribution from exchange and overlap effects is essentially zero and the potential is entirely due to the van der Waals tail:

$$-(C_6/r^6+C_8/r^8+C_{10}/r^{10}) .$$

TABLE II. Spectroscopy results for several argon potentials. Deviations of the predictions of various potentials from the (a) vibrational spacings ΔG and (b) rotational constants B_v of the argon dimer determined by vacuum ultraviolet laser spectroscopy [Herman *et al.*, J. Chem. Phys. **89**, 4535 (1988)]. Units of cm^{-1}.

(a) Vibrational spacings

	Experimental energy spacing (cm^{-1})	Estimated error (cm^{-1})	Deviations from experiment (cm^{-1})			
			HFDID1	MMS-1[a]	MMS-2[a]	MHFD[a]
$G(\frac{3}{2})$-$G(\frac{1}{2})$	25.69	0.02	0.014	−1.379	−1.455	−0.657
$G(\frac{5}{2})$-$G(\frac{3}{2})$	20.58	0.02	−0.023	−1.413	−1.533	−1.249
$G(\frac{7}{2})$-$G(\frac{5}{2})$	15.58	0.02	−0.004	−1.252	−1.212	−1.369
$G(\frac{9}{2})$-$G(\frac{7}{2})$	10.91	0.03	0.010	−0.955	−0.653	−1.144
$G(\frac{11}{2})$-$G(\frac{9}{2})$	6.84	0.07	−0.013	−0.624	−0.076	−0.781
$G(\frac{11}{2})$-$G(\frac{1}{2})$	79.57	0.09	0.014	−5.605	−4.914	−5.170

(b) Rotational constants

	Experimental B_v Values	Error bars	Deviations from experiment			
v			HFDID1	MMS-1[a]	MMS-2[a]	MHFD[a]
0	0.057 76	0.000 06	+0.000 01	−0.000 90	−0.000 95	−0.001 90
1	0.053 48	0.000 07	−0.000 05	−0.001 33	−0.001 47	−0.001 02
2	0.048 61	0.000 09	−0.000 08	−0.002 57	−0.002 69	−0.002 44
3	0.043 03	0.000 12	−0.000 12	−0.001 77	−0.001 70	−0.001 84
4	0.036 74	0.000 39	−0.000 32	−0.001 90	−0.001 41	−0.002 08
5	0.030 36	0.000 65	−0.001 37	−0.002 72	−0.001 56	−0.002 98

[a]Mimics of the FVVMCB potential.

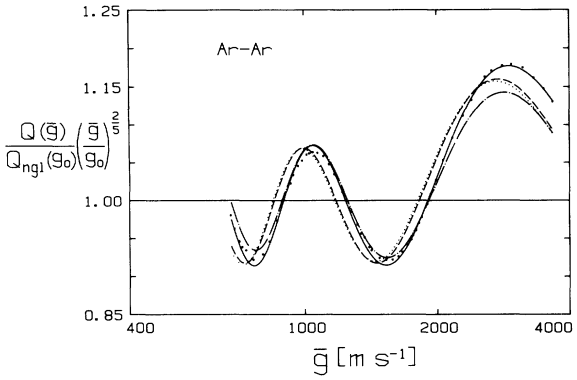

FIG. 3. Comparison of the experimental total collision cross section data of van den Biesen *et al.* (Ref. [16]) (large dots) with the cross sections calculated on the basis of the HFDID1 (solid line), the MMS-1 (dashed line), the MMS-2 (dash-dotted line), and the MHFD (dotted line) potentials.

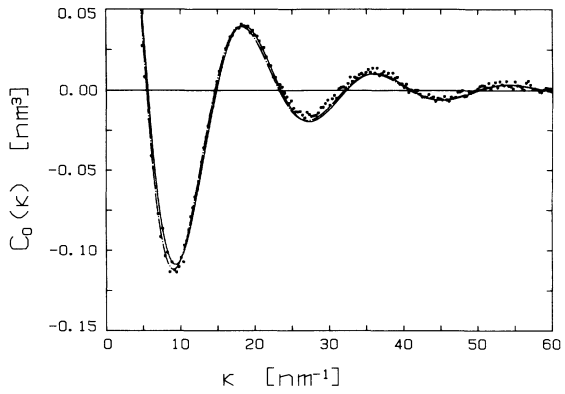

FIG. 4. $C_0(\kappa)$ of Fredrikze *et al.* (large dots) and those calculated from potentials HFDID1 (solid line) and the MMS-2 (dash-dotted line).

If one inputs the maximum allowable values of the dispersion coefficients [13,14] into this expression, one obtains for the maximum depth a value of $u(1.6\sigma) = -24.8$ K, which is 11.8% *less shallow* than $u_{\text{MMS-2}}(1.6\sigma)$.

Another property which is a good discriminator of potentials is the *PVT* second virial coefficient. This property as a function of temperature (room to lower temperatures) senses the area of the well and, in a way, its well depth. Maximum deviations (positive and negative) on the basis of the four potentials from various sets of experimental data [17–19] are presented in Table III. The table shows that none of the mimic potentials can predict the second virial data. However, the HFDID1 [11] predicts the virial data quite well.

Another good discriminator for potentials is the glory structure in the TCCS [16]. This property senses the potential from just inside the potential minimum to long range. It places stringent constraints on the shape of the well, the long-range behavior and the product of the well depth ϵ and the length parameter r_m. The glory structure in the TCCS was determined on the basis of the three mimic and the HFDID1 potentials and compared to the data of van den Biesen, Hermans, and van den Meijdenberg [16] in the form of a plot shown in Fig. 3. From this figure, it is seen that only the HFDID1 predicts the experimental TCCS data satisfactorily.

Finally, we calculated the Fourier transform $C_0(\kappa)$ of the direct correlation function $c_0(r)$ in the limit of zero density for the range $2.4 \leq \kappa \leq 100$ on the basis of the HFDID1, MMS-1, MMS-2, and MHFD potentials and compared them with the experimental data of Fredrikze *et al.* [20]. In Table IV, we indicate the percentage of experimental data points that are predicted within their respective errors by each of the three mimic and HFDID1 potentials and the corresponding rms deviations. The Fourier transform $C_0(\kappa)$ on the basis of the HFDID1 and the three mimic potentials are plotted in Figs. 4 and 5 as a function of κ along with the "experimental" values.

DISCUSSION

The HFDID1 argon potential of Aziz [11] was constructed by incorporating the best *ab initio* results at short and long range into a realistic potential function form and then determining its adjustable parameters by fitting the function to a judiciously selected set of experimental data. It is then able to reproduce those data and to predict a variety of other properties over a large temperature/energy range within the accuracy of the data. This potential appears to be the best characterization of the Ar-Ar interaction produced to date. The HFD-*B*2 [5] and HFD-*B*3 [6] are almost as good.

However, pair potentials derived from neutron diffraction experiments suffer from several defects. The long- and short-range portions of the diffraction potentials cannot be determined directly, so one often does not know the potential over all the separations which might be of interest. Most notably, no information about the repulsive wall of the potential is available. Even within the region of the potential bowl, i.e., where $u_2(r)$ is nega-

TABLE III. Maximum deviations of several potentials from second virial data.

Second virial coefficient	Temperature range (K)	Error bars (ml mol^{-1})	Potential HFDID1 (ml mol^{-1})	MMS-1 (ml mol^{-1})	MMS-2 (ml mol^{-1})	MHFD (ml mol^{-1})
Michels *et al.* [17]	133–248	±0.3	+0.18	+7.87	−6.57	10.81
Michels *et al.* [18]	273–423	±0.3	−0.20	+3.46	−2.50	4.65
Hahn *et al.* [19]	200–273	±2	+0.26	+4.40	−4.24	6.12

TABLE IV. Comparison of experimental and calculated values of $C_0(\kappa)$, the low-density limit of the Fourier transform of the direct correlation function $c_0(r)$.

	Deviations from experiment			
	HFDID1	MMS-1	MMS-2	MHFD
rms deviation (nm^3)	0.0060	0.029	0.0054	0.0029
Percentage of calculated points within error bars	45.0	47.7	48.8	48.5

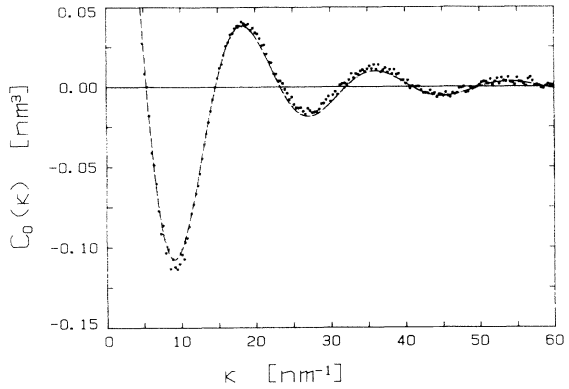

FIG. 5. $C_0(\kappa)$ of Fredrikze *et al.* (large dots) and those calculated from potentials MMS-1 (dashed line) and the MHFD (dotted line).

tive, the precise value of $u_2(r)$ at any particular r is not readily determined since the potentials tend to be presented in graphical or tabular form rather than analytical form. In particular, each of the three mimics of the FVVMCB argon potential of Fredrikze *et al.* are *shallower* near the well minimum but *deeper* at larger separations than currently accepted potentials. The MMS-1 and MHFD have smaller well areas while the MMS-2 has a larger area than the HFDID1 potential. These factors lead to shapes which are different in general, namely, shallower at the well minimum, narrower near the bottom and wider near the top of the well. As a result, poor predictions for properties which are influenced entirely or chiefly by the potential well like spectroscopic, low and room temperature virials and total cross section data can be expected and do occur. Additionally, as shown in Table IV, all four potentials are essentially equivalent in their ability to reproduce the $C_0(\kappa)$ values within the estimated error bars despite their substantial differences in shape. This shows the insensitivity of this property to the potential. Also, the three mimic potentials do not reproduce the data from which they were derived. This indicates a possible problem with the inversion technique or the accuracy of the data or both.

CONCLUSION

In conclusion, we note that potentials inverted from diffraction data tend to produce the approximate shape of the potential in the region of the bowl. Nevertheless, they should not be regarded as accurate representations of the pair interaction. The associated errors of the inverted numerical potential are large and as such can give rise to a large number of possible potentials which have a variety of shapes but which still lie within the quoted errors. None of these potentials of different shape can be expected to predict the spectroscopic data; the shallow well depth alone would rule out each as a proper characterization of the interaction. We also note that both spectroscopic data and theoretical considerations rule out the premise that the potential is about 15% deeper near $r=1.6\sigma$, where one has most confidence in the data [2,21]. For the rare gases, the inversion of a single property whether it be microscopic (differential or total cross sections or spectroscopy) or macroscopic (*PVT* second virial coefficients or viscosity, etc.) has never yielded a sufficiently accurate potential. The best procedure to date is a multiproperty fit of a suitably realistic potential form to a judiciously selected set of data. The reason is that a specific property senses the potential in a specific region and the set of properties chosen must constrain the potential over a large range of separations.

ACKNOWLEDGMENT

Financial support for this project was provided by the Natural Sciences and Engineering Research Council of Canada.

APPENDIX

(i) The form of the (reduced) Maitland-Smith potential is

$$u_2^*(x)=(n-6)^{-1}[6/x^n-n/x^6] ,$$

where $n=\alpha+\gamma(x-1)$. In the hybrid version, the values of parameters α and γ in the region $x<1$ can differ from their values when $x\geq 1$. For $x<1$, $\alpha=\alpha_1$, $\gamma=\gamma_1$, and for $x\geq 1$, $\alpha=\alpha_2$, $\gamma=\gamma_2$. (ii) The form of the HFD-*B* potential is

$$U(r)=\epsilon U^*(x) ,$$

where

$$U^*(x)=A^*\exp(-\alpha^* x+\beta^* x^2) - F(x)\{c_6/x^6+c_8/x^8+c_{10}/x^{10}\}$$

with

$$F(x)=\begin{cases}\exp[-(D/x-1)^2] , & x<D \\ 1 , & x\geq D .\end{cases}$$

[1] C. D. Andriesse and E. Legrand, Physica **57**, 191 (1972).
[2] F. Barocchi, M. Zoppi, and P. A. Egelstaff, Phys. Rev. A **31**, 2732 (1985).
[3] H. Fredrikze, J. B. van Tricht, A. A. van Well, R. Magli, P. Chieux, and F. Barocchi, Phys. Rev. Lett. **62**, 2612 (1989); H. Fredrikze (private communication).
[4] J. A. Barker, R. A. Fisher, and R. O. Watts, Mol. Phys. **21**, 657 (1971).
[5] R. A. Aziz and M. J. Slaman, Mol. Phys. **58**, 679 (1986).
[6] R. A. Aziz and M. J. Slaman, J. Chem. Phys. **92**, 1030 (1990).
[7] J. M. Parson, P. E. Siska, and Y. T. Lee, J. Chem. Phys. **56**, 1511 (1972).
[8] R. A. Aziz and H. H. Chen, J. Chem. Phys. **67**, 5719 (1977).
[9] A. Koide, W. J. Meath, and A. R. Allnatt, Mol. Phys. **39**, 895 (1980).
[10] C. Douketis, G. Scoles, S. Marchetti, M. Zen, and A. J. Thakkar, J. Chem. Phys. **76**, 3057 (1982).
[11] R. A. Aziz, J. Chem. Phys. **99**, 4518 (1993).
[12] G. C. Maitland and E. B. Smith, Chem. Phys. Lett. **22**, 443 (1973).
[13] A. Kumar and W. J. Meath, Mol. Phys. **54**, 823 (1985).
[14] J. M. Standard and P. R. Certain, J. Chem. Phys. **83**, 3002 (1985).
[15] P. R. Herman, P. E. LaRocque, and B. P. Stoicheff, J. Chem. Phys. **89**, 4535 (1988).
[16] J. J. van den Biesen, R. M. Hermans, and C. J. N. van den Meijdenberg, Physica A **115**, 396 (1982).
[17] A. Michels, J. M. Levelt, and W. de Graaf, Physica **24**, 659 (1958).
[18] A. Michels, Hub. Wijker, and Hk. Wijker, Physica **15**, 627 (1949).
[19] R. Hahn, K. Schaefer, and B. Schramm, Ber. Bunsenges Phys. Chem. **78**, 287 (1974).
[20] H. Fredrikze (private communication).
[21] P. Egelstaff (private communication).